International Journal of Electrical Components and Energy Conversion
2016; 2(4): 21-34
http://www.sciencepublishinggroup.com/j/ijecec
doi: 10.11648/j.ijecec.20160204.11
ISSN: 2469-8040 (Print); ISSN: 2469-8059 (Online)

Validating Response of ac Micro-grid to Three Phase Short Circuit in Grid-Connected Mode Using Dynamic Analysis

Maruf A. Aminu

Department of Electrical and Computer Engineering, Curtin University, Sarawak, Malaysia

Email address:
maruf.aminu@gmail.com

To cite this article:
Maruf A. Aminu. Validating Response of ac Micro-grid to Three Phase Short Circuit in Grid-Connected Mode Using Dynamic Analysis. *International Journal of Electrical Components and Energy Conversion.* Vol. 2, No. 4, 2016, pp. 21-34. doi: 10.11648/j.ijecec.20160204.11

Received: April 1, 2016; **Accepted**: February 24, 2017; **Published**: March 11, 2017

Abstract: This paper presents the results of attempt to validate the response dynamism of an 11kW, 575V wind turbine micro-grid connected to a 100MVA, 13.8kV utility under three phase bolted short circuit. The micro-grid was modeled using two Doubly-Fed Induction Generators (DFIGs). The test bed was developed in SimPowerSystems® at a system frequency of 50Hz with cut-in and cut-out wind speeds of $3ms^{-1}$ and $6ms^{-1}$, respectively. Short circuit fault is applied at 6.0s and withdrawn at 8.0s, and 50.0s dynamic response of the system is obtained for different fault locations, under voltage and reactive power controls of the wind turbine controller in grid-connected mode. The results of the study show bidirectional power flow due to power exchange between the utility and micro-grid, and poor post-fault sub-transient and transient instability associated with the micro-grid due to comparatively lower inertia. The study also shows that the micro-grid presents superior performance when stressed under Q control than under V control. Finally, the response of the test bed is found to be consistent with established short circuit theory, establishing its validity.

Keywords: Micro-grid, Dynamic, DFIG, Micro-source, Fault

1. Introduction

A power system is designed to generate electric power in sufficient quantity and on continuous basis to meet the present and forecasted future demands of the users in an area, and to transmit power generated to the areas where it will be utilized and then distribute it within that area. To achieve this, the whole system must be kept in operation continuously without major breakdowns. This can only be achieved, practically, through use of protective devices [1]. The protective devices ensure:

1. Minimal damage and repair costs whenever they sense fault.
2. Safeguard of the entire power system to maintain continuity of supply.
3. Safety of personnel.

In order to meet above requirements, short circuit analysis must be performed on the power system at the design stage to determine the short circuit rating of new switchgear and other substation infrastructure equipment that will be purchased, installed and commissioned. Similarly, manufacturers of power system switchgear and substation infrastructure equipment, e.g. generators, transformers and cables, use the short circuit ratings specified by their clients to ensure that the equipment is designed to safely withstand the flow of these currents for a specified duration [2-4]. As the critical parameters of a power system and fault envelopes vary with time [5-7], an analysis which depicts the dynamism of the system under short circuit is veritable to achieving operational goals of a power system - ensuring continuous, high quality and safe delivery of power to consumers.

The test bed presented in this paper was developed as a working platform for a study which seeks to propose a new relay for micro-grids. Either DFIG in the test bed is nominally rated 5.5kW and linked to 2.5km highly resistive feeder (a or b), radially interconnected to the utility at the Point of Common Coupling (PCC). A 20MVA STATCOM was modeled and connected at the PCC. While the utility services a local 3.6MVA and a remote 89.44MVA inductive loads, the micro-grid has total inductive local load of 6.21kVA. The anticipated protective system would be based on measurement of three phase power. Therefore, three phase nominal active and reactive power is investigated and presented in this study. Since the validity of the anticipated

relay depends on the validity of the test bed's response, this work is performed to establish the validity of the test bed under three phase balanced bolted short circuit.

2. Characterization of Three Phase Short Circuit

In a generator, fault current is initially around 8 times full-load current. It decays rapidly to around 5 times full-load current before decaying less rapidly to less than full-load current value. These three stages of fault current envelop in the direct axis are called sub-transient $(X_d^{"})$, transient $(X_d^{'})$ and steady-state (X_d) respectively. At no load, the electromagnetic force (e.m.f.) is same as the system voltage, V, which at the nominal value is 1.0 pu. At any other load the e. m. f. is greater than at no load and given by (1) to (3). Consequently, in increasing magnitude, the direct-axis reactances are

$$(X_d^{"}) < (X_d^{'}) < (X_d) \tag{1}$$

$$E^{"} = [(V + X_d^{"} I \sin\varphi)^2 + (X_d^{"} I \cos\varphi)^2]^{\frac{1}{2}} \tag{2}$$

$$E = [(V + X_d I \sin\varphi)^2 + (X_d I \cos\varphi)^2]^{\frac{1}{2}} \tag{3}$$

While the current associated with (3) is a steady value, the current associated with (2) is an initial value at the onset of short circuit. The sub-transient value decays in a fraction of a second while the transient value takes several seconds to decay. The open-circuit sub-transient time constant $(T_{d0}^{"})$ and transient time constant $(T_{d0}^{'})$ are typically 0.1s and 5.0s, respectively [8-12].

3. Short Circuit in a Power System

Consider a three phase-to-earth fault at point F2 as shown in Figure 1. In Figure 1, G1 and G2 are generators. CB1 to CB4 are circuit breakers, while F1 to F3 are short circuit points. L is a load connection.

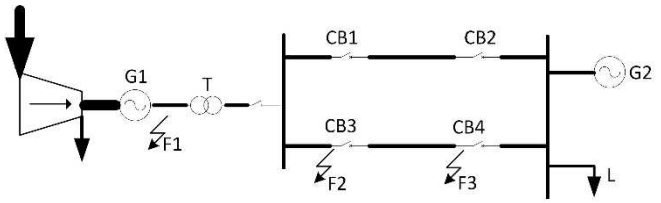

Figure 1. *Typical power system with short circuit points F1, F2 and F3.*

It is accurate to view fault F2 as a modified generator fault which includes the effect of transformer T. The transformer reactance, X_T, is added to the reactance $X_d^{"}$, $X_d^{'}$ and X_d as given in (4), (5) and (6) [13-17].

$$x_d^{"} = X_d^{"} + X_T \tag{4}$$

$$x_d^{'} = X_d^{'} + X_T \tag{5}$$

$$x_d = X_d + X_T \tag{6}$$

The amplitude of the ac fault current in the sub-transient state, $i_m^{"}$, transient state, $i_m^{'}$, and steady state, i_m^{∞}, is presented in (7), (8) and (9), respectively. E_{fm} is the amplitude value of e.m.f.

$$i_m^{"} = \frac{E_{fm}}{x_d^{"}} \tag{7}$$

$$i_m^{'} = \frac{E_{fm}}{x_d^{'}} \tag{8}$$

$$i_m^{\infty} = \frac{E_{fm}}{x_d} \tag{9}$$

Addition of X_T attenuates the magnitude of the currents given in (7), (8) and (9). Secondly, the transformer resistance, R_T, speeds up the rate of dissipation of the stored magnetic energy so that the short circuit current (dc component) decays more rapidly. Thirdly, the transformer reactance increases the time constants as given in (10) and (11) [18-20].

$$T_{d(network)}^{"} = T_d^{"} \left(\frac{X_d^{'}}{X_d^{"}} \right) \left(\frac{X_d^{"} + X_T}{X_d^{'} + X_T} \right) \tag{10}$$

$$T_{d(network)}^{'} = T_d^{'} \left(\frac{X_d}{X_d^{'}} \right) \left(\frac{X_d^{'} + X_T}{X_d + X_T} \right) \tag{11}$$

4. Design of Control Systems

In practice, power system protection cannot be excluded from the effects of control devices [21]. The test bed under study was subjected to time-domain step response analysis. It was found to be stable but its response was poor. Then, regulators were designed in closed-loop feedback architecture. The systems designed are pitch angle regulator, active power regulator, reactive power regulator, grid ac voltage regulator, dc bus voltage regulator, grid-side converter current regulator and rotor-side converter current regulator. The test bed was then subjected to another small signal analysis and found to be stable with satisfactory response. Two mutually exclusive control regimes were then implemented by appropriate combination of the regulators. The control regimes are the active power-voltage (*PV* or *V*) control and the active-reactive power (*PQ* or *Q*) control [22]. When the micro-grid is operated in *V* control, the voltage controller maintains the grid voltage constant with a 4% droop. When it is operated in *Q* control, the var controller maintains the reactive power at the grid constant by injecting or absorbing reactive power.

5. Short Circuit Simulation and System Dynamic Response

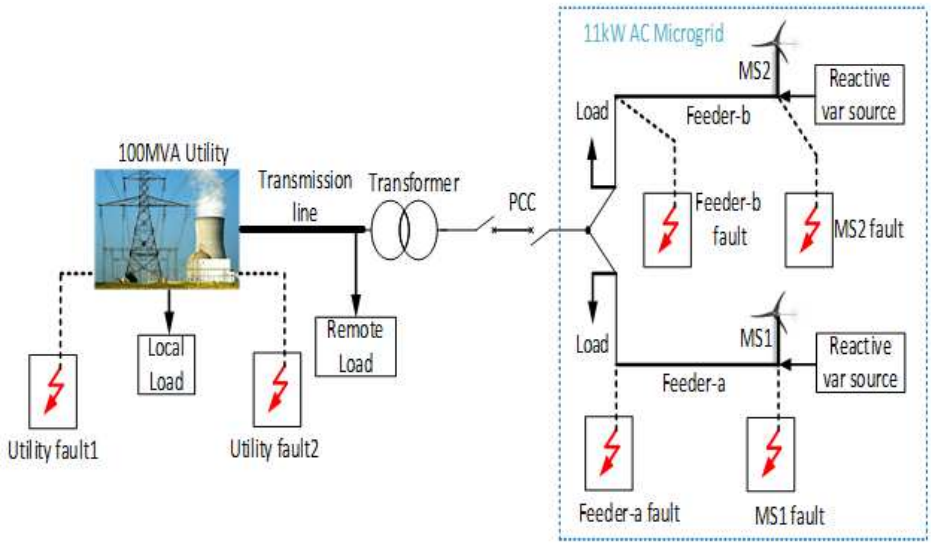

Figure 2. *A simplified schematic diagram for the system under investigation.*

The test bed developed for this study is shown in Figure 2.
Figure 3 shows the response of the micro grid during normal operation under *V* and *Q* controls.

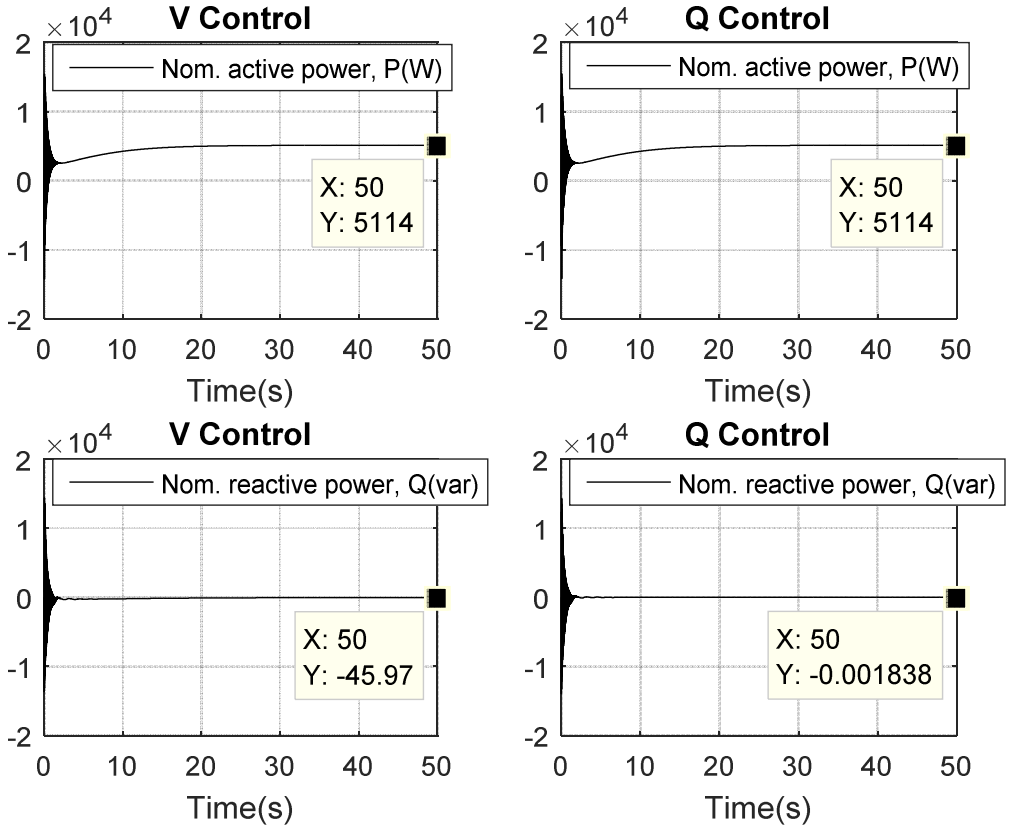

Figure 3. *Response of micro grid under normal operation in V and Q Controls.*

Three phase-to-earth bolted short-circuit fault is applied at 6.0s and withdrawn at 8.0s. Dynamic simulation of the test bed (synch. generator, micro grid feeders and DFIG) under short circuit is performed for 50.00s. The responses of the test bed for different fault locations and DFIG controller in *V* and *Q* controls are presented in Figure 4(a) to Figure 12(b).

The responses of MS1 under *V* and *Q* controls when utility generator terminals are short-circuited are presented in Figure 4(a) and Figure 4(b), respectively.

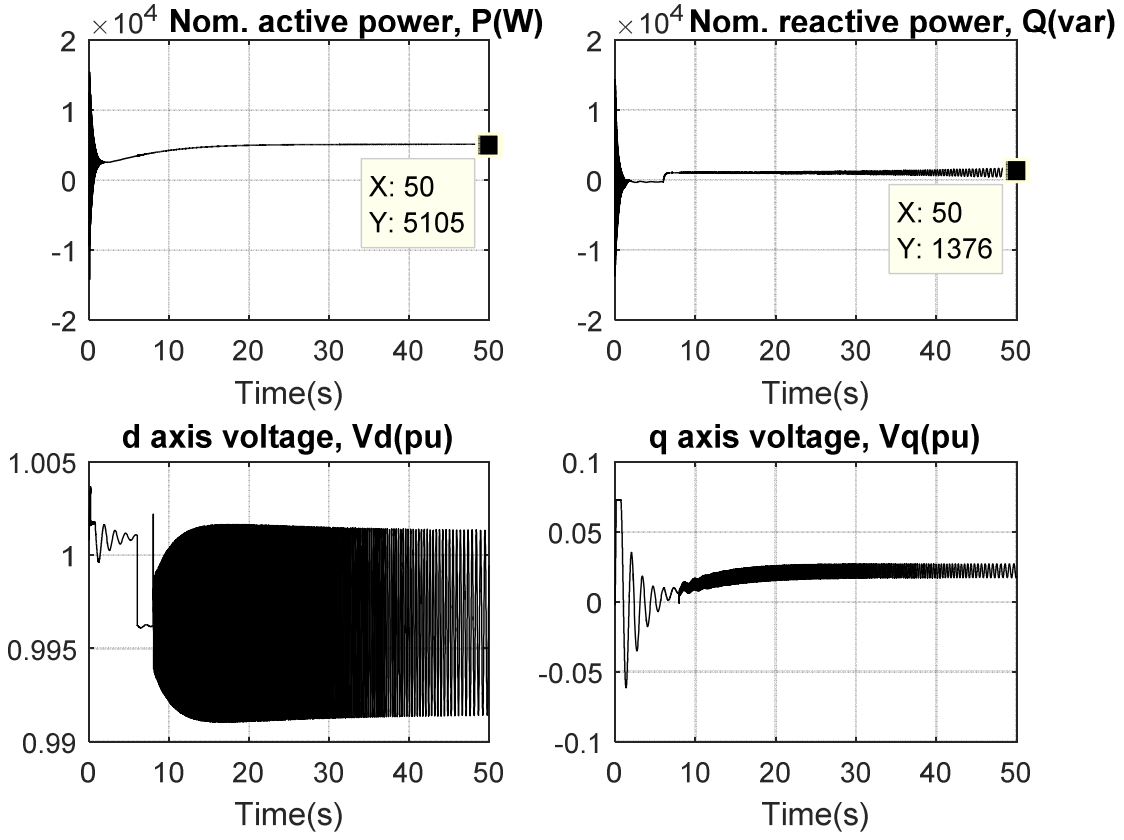

Figure 4(a). *Response of MS1 when utility generator terminals are short-circuited at 6.0s to 8.0s - V Control.*

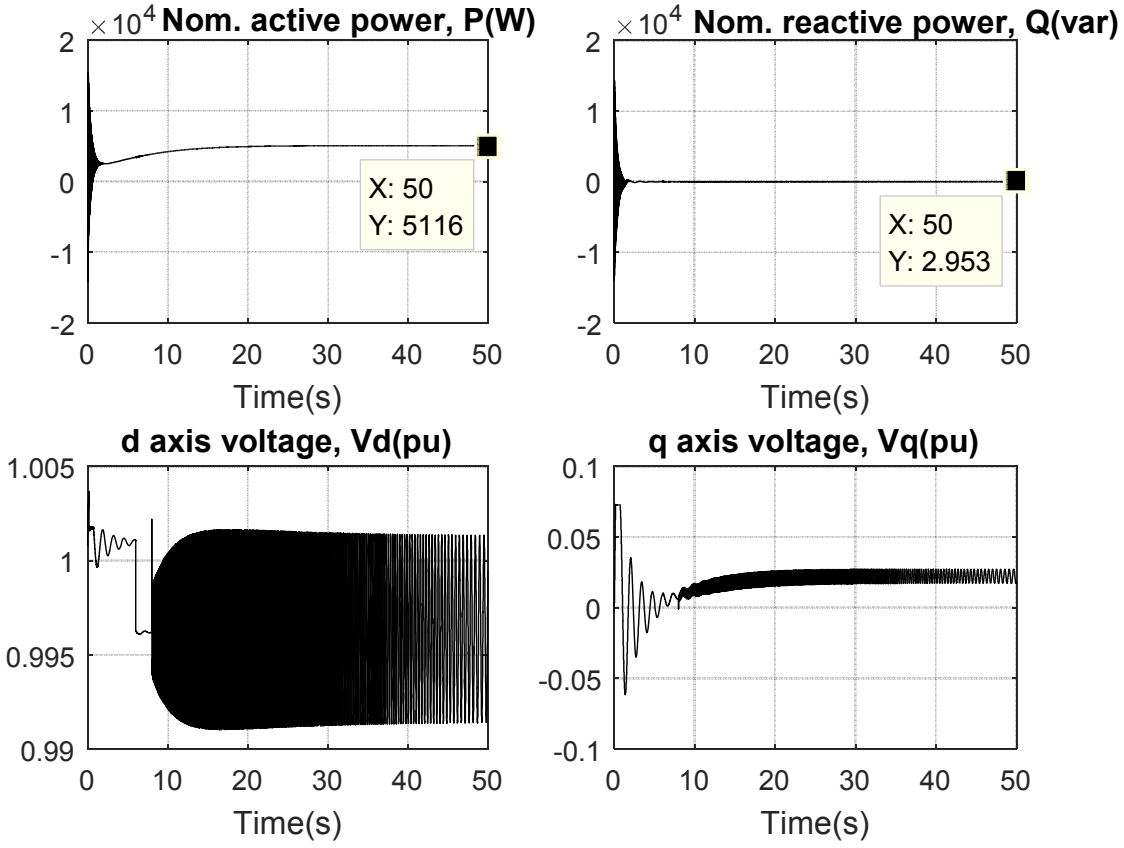

Figure 4(b). *Response of MS1 when utility generator terminals are short-circuited at 6.0s to 8.0s - Q Control.*

Figure 5(a) and Figure 5(b) present responses of feeder-a to faults at the terminals of utility generator, respectively.

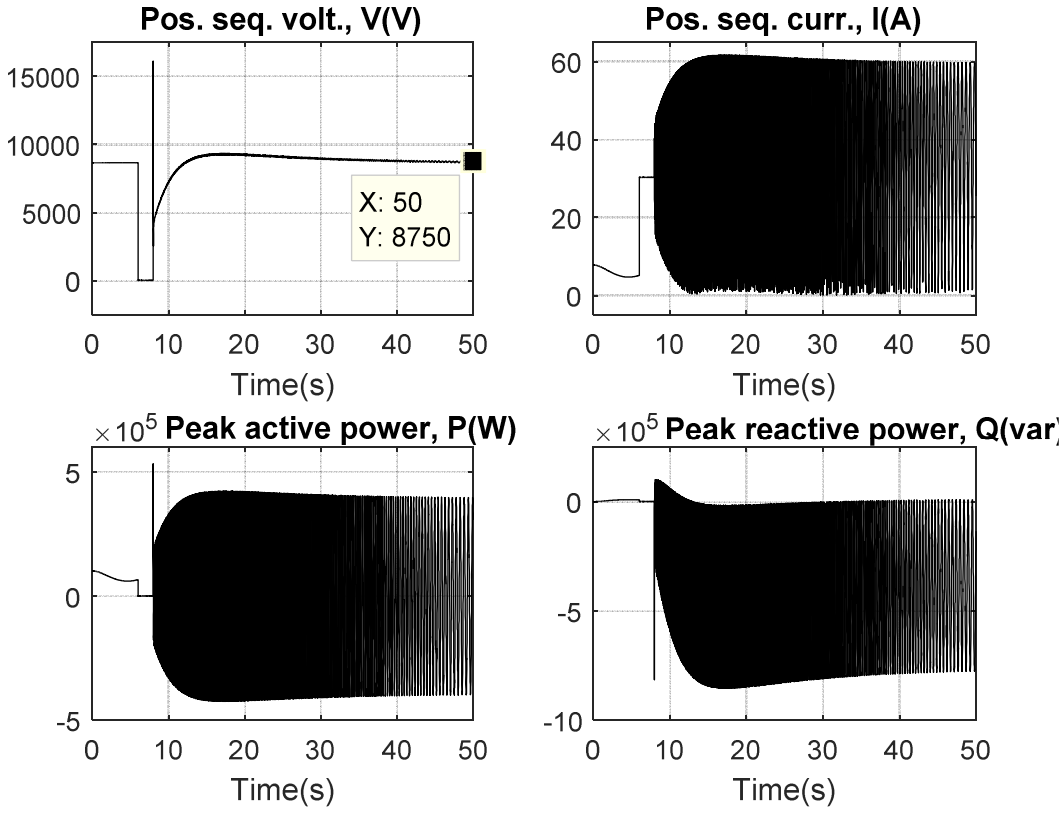

Figure 5(a). *Response of feeder-a when utility generator terminals are short-circuited at 6.0s to 8.0s - V Control.*

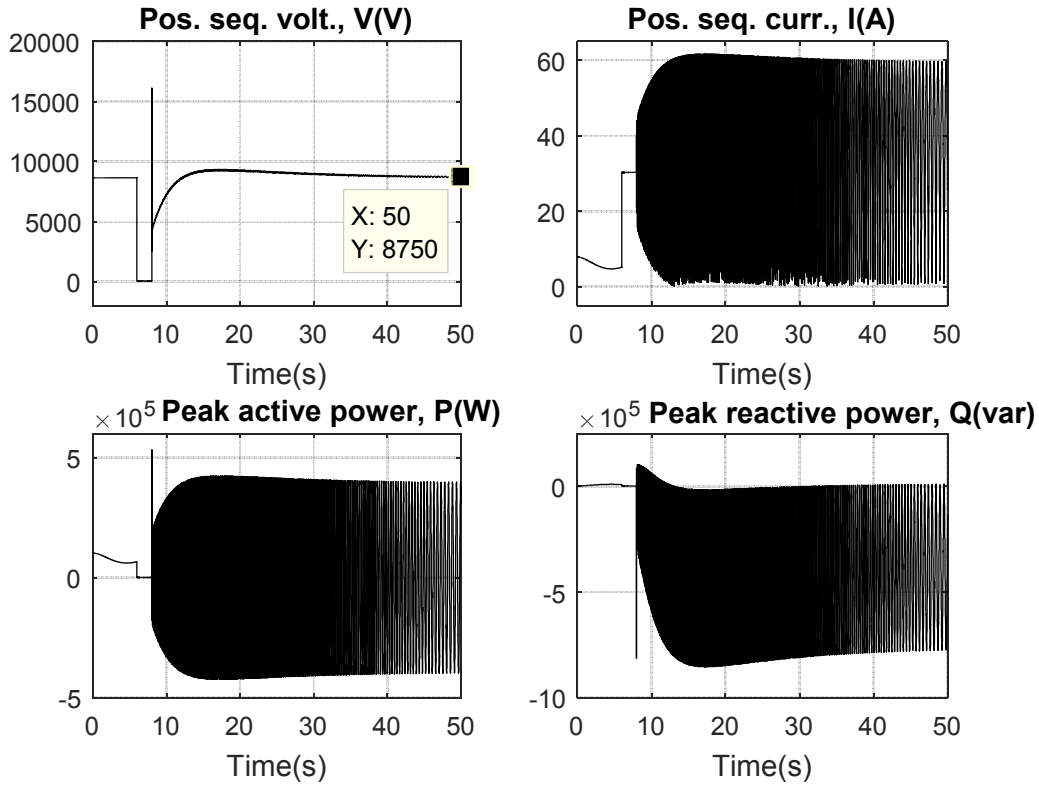

Figure 5(b). *Response of feeder-a when utility generator terminals are short-circuited at 6.0s to 8.0s - Q Control.*

The responses of MS1 under *V* and *Q* controls when ends of transmission lines are short-circuited are presented in Figure 6(a) and Figure 6(b), respectively.

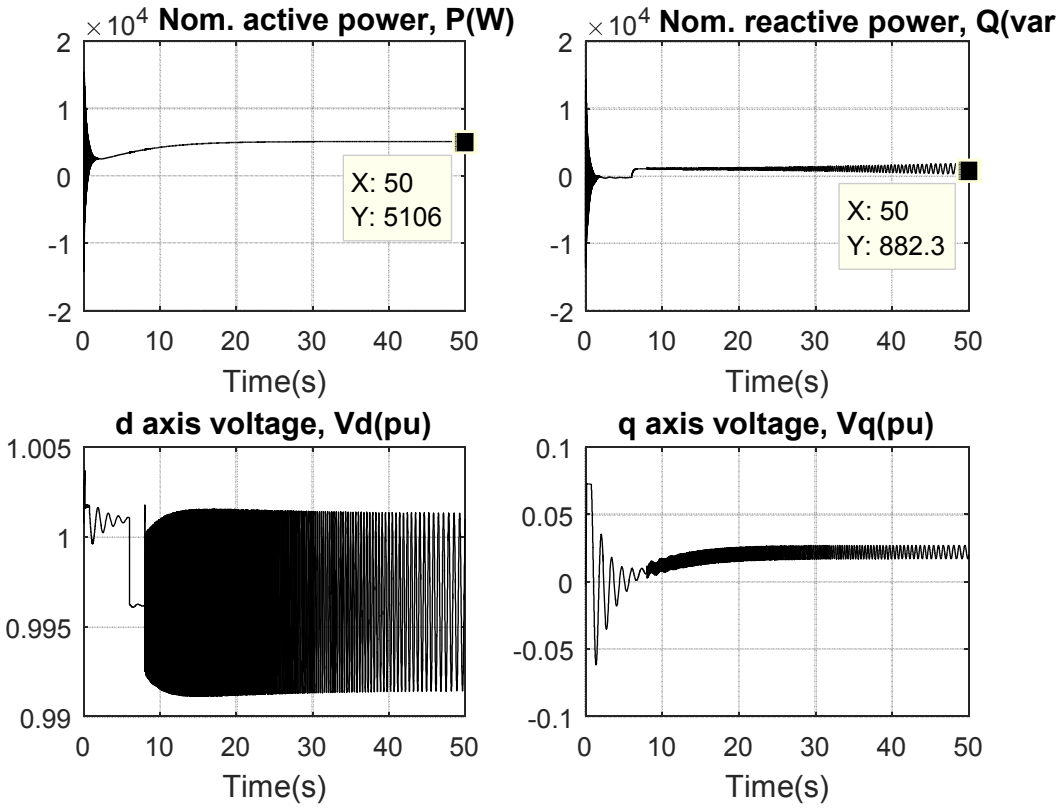

Figure 6(a). *Response of MS1 when ends of transmission lines are short-circuited at 6.0s to 8.0s - V Control.*

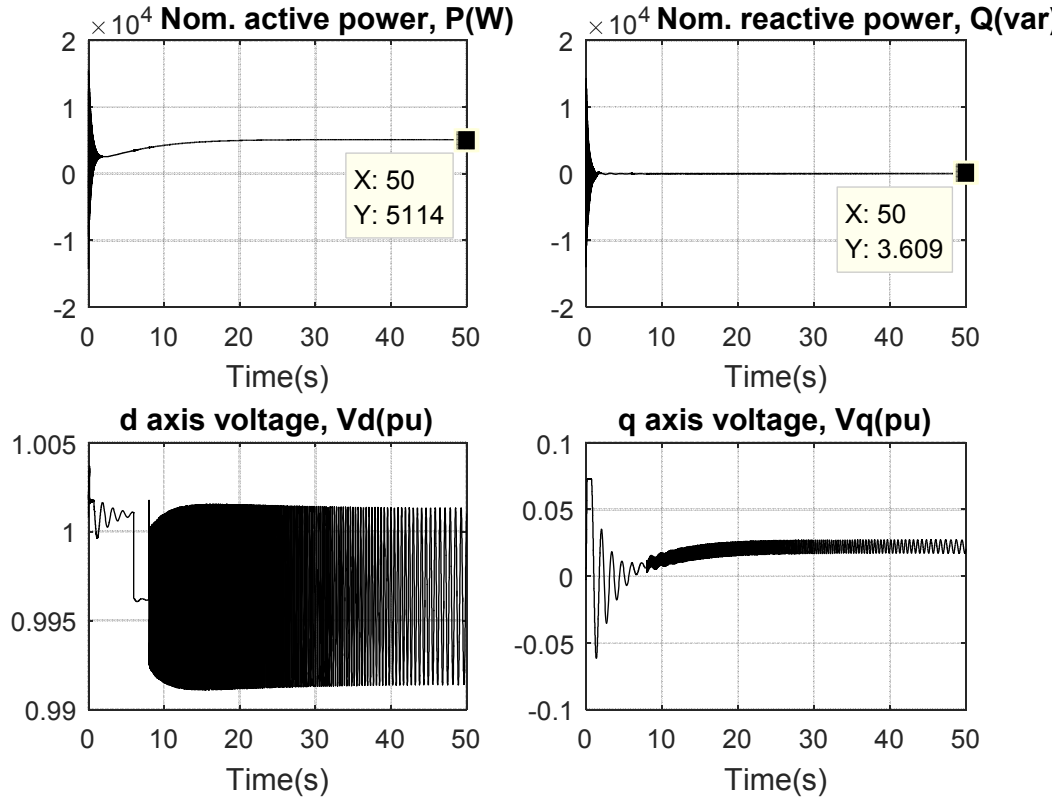

Figure 6(b). *Response of MS1 when ends of transmission lines are short-circuited at 6.0s to 8.0s - Q Control.*

Figure 7(a) and Figure 7(b) present responses of feeder-a to faults at the ends of transmission lines (closer to the micro-grid) under *V* and *Q* controls, respectively.

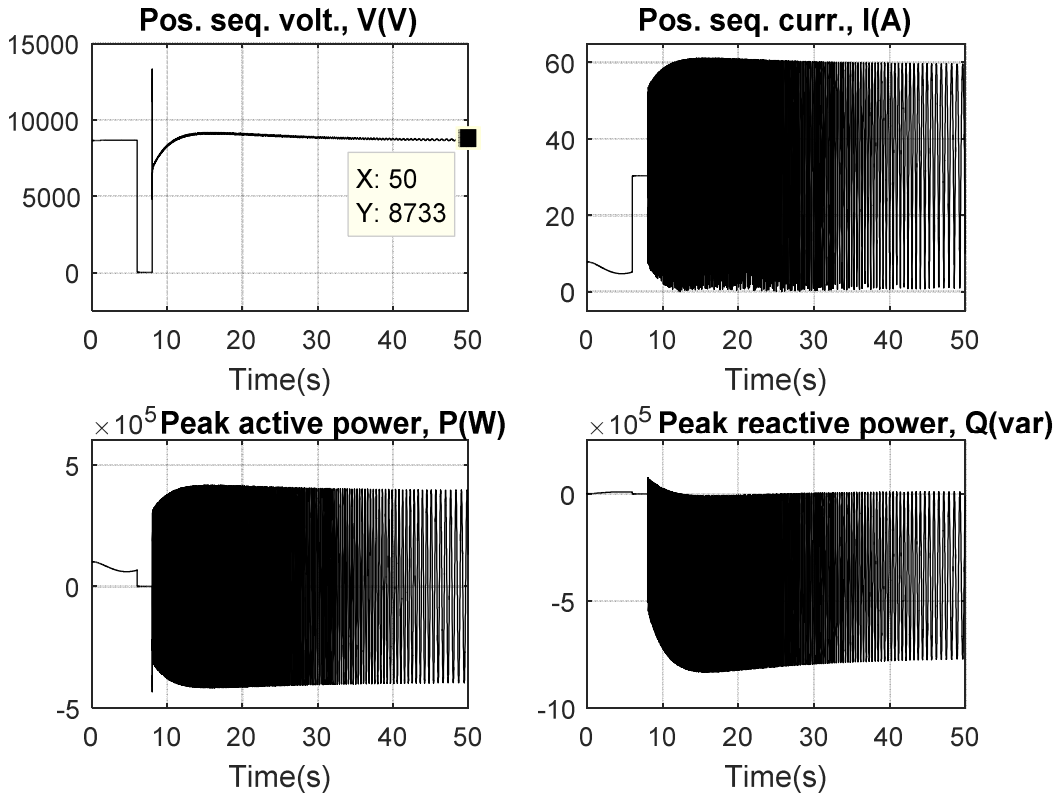

Figure 7(a). *Response of feeder-a when ends of transmission lines are short-circuited at 6.0s to 8.0s - V Control.*

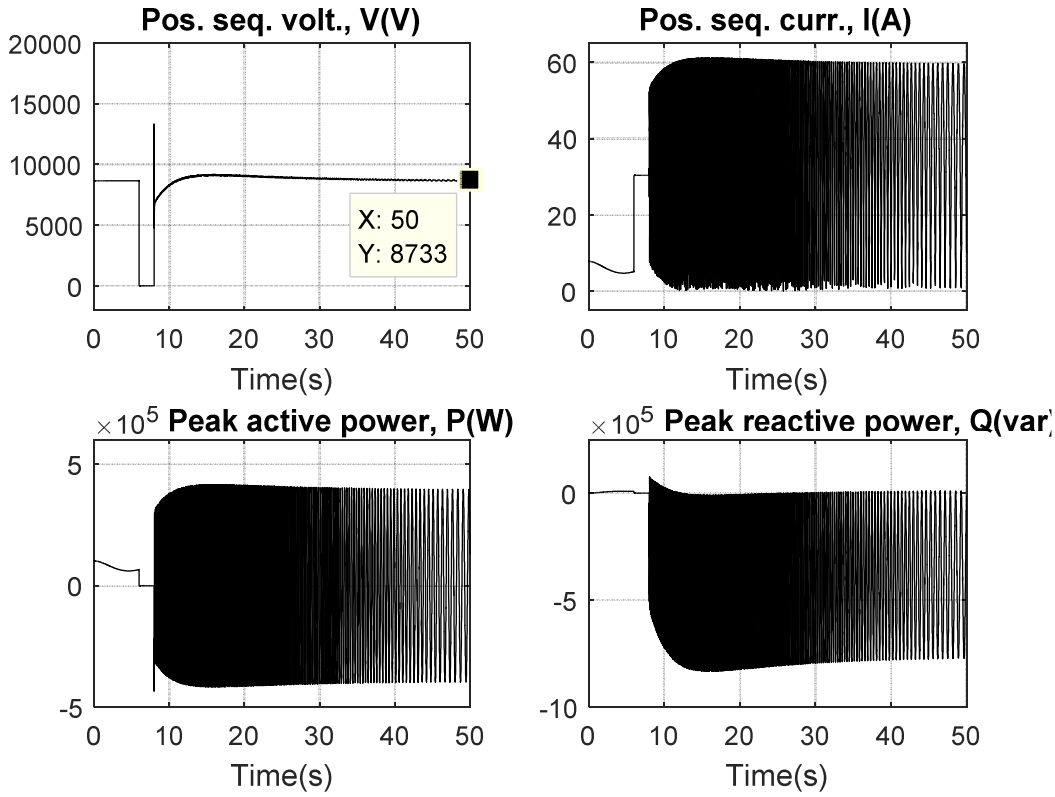

Figure 7(b). *Response of feeder-a when ends of transmission lines are short-circuited at 6.0s to 8.0s - Q Control.*

The responses of MS1 under *V* and *Q* controls when its terminals are short-circuited are presented in Figure 8(a) and Figure 8(b), respectively.

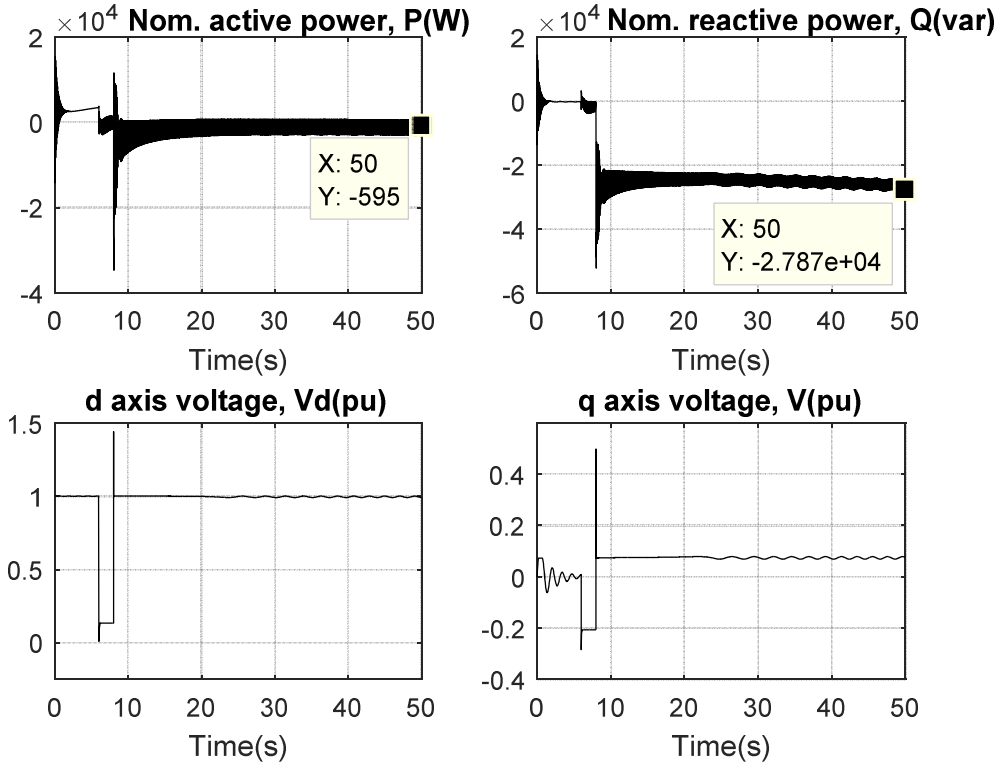

Figure 8(a). *Response of MS1 when its terminals are short-circuited at 6.0s to 8.0s - V Control.*

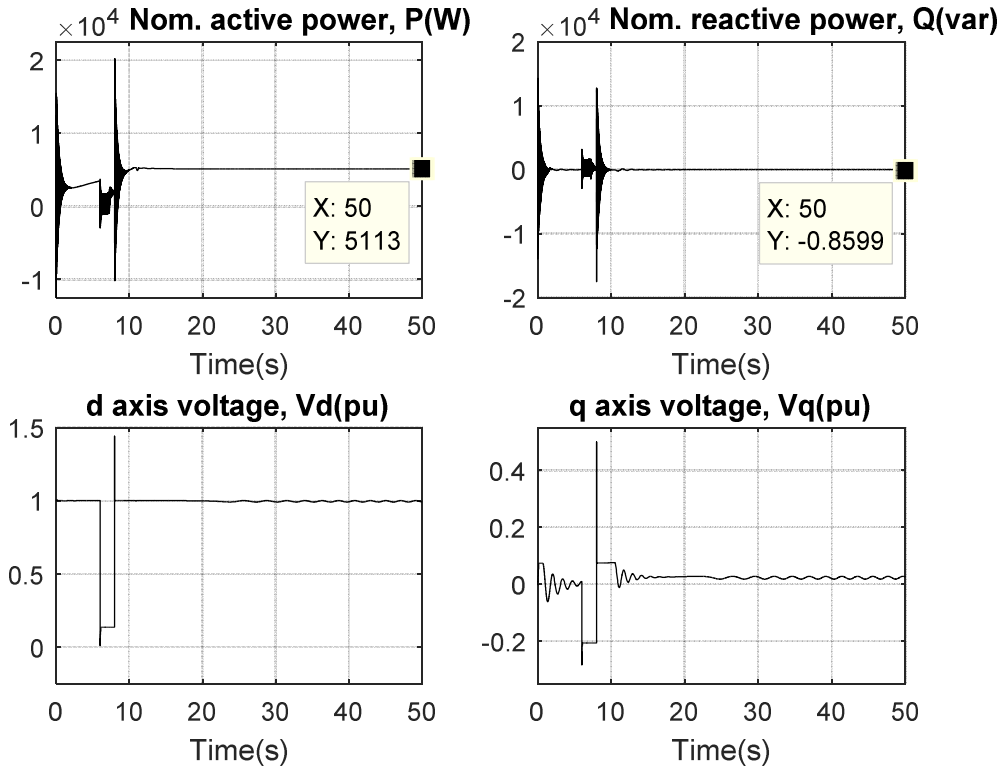

Figure 8(b). *Response of MS1 when its terminals are short-circuited at 6.0s to 8.0s - Q Control.*

The responses of MS2 under *V* and *Q* controls when terminals of MS1 are short-circuited are presented in Figure 9(a) and Figure 9(b), respectively.

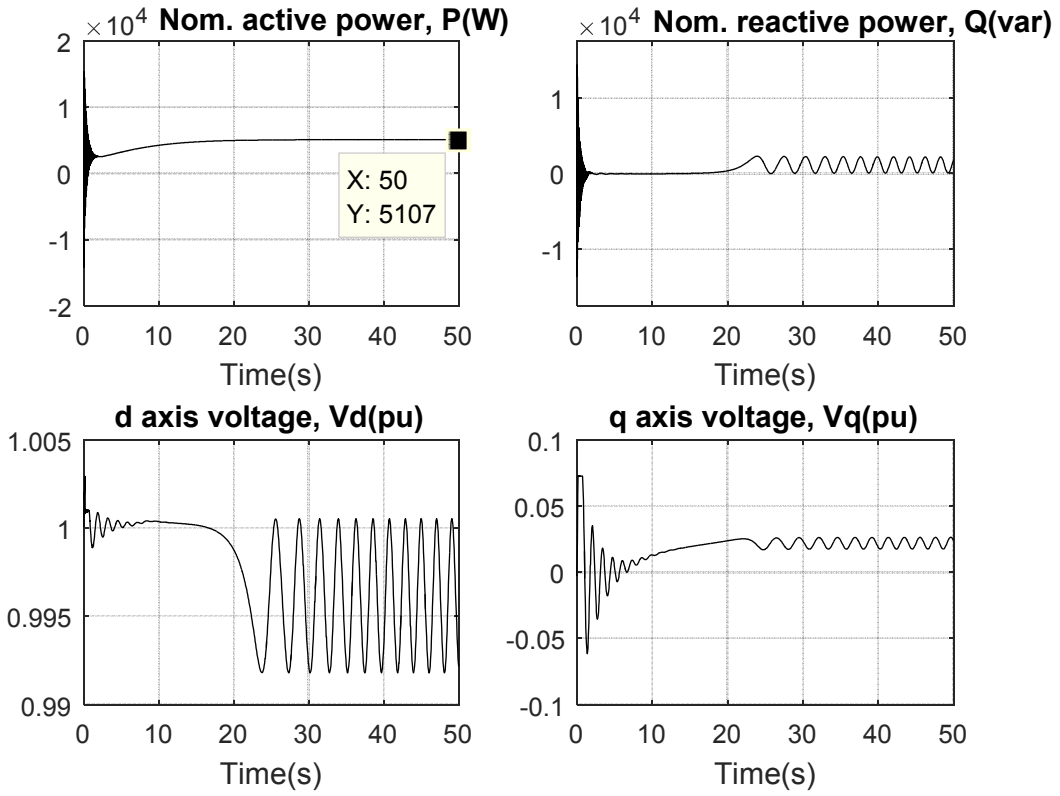

Figure 9(a). *Response of MS2 when terminals of MS1 are short-circuited at 6.0s to 8.0s - V Control.*

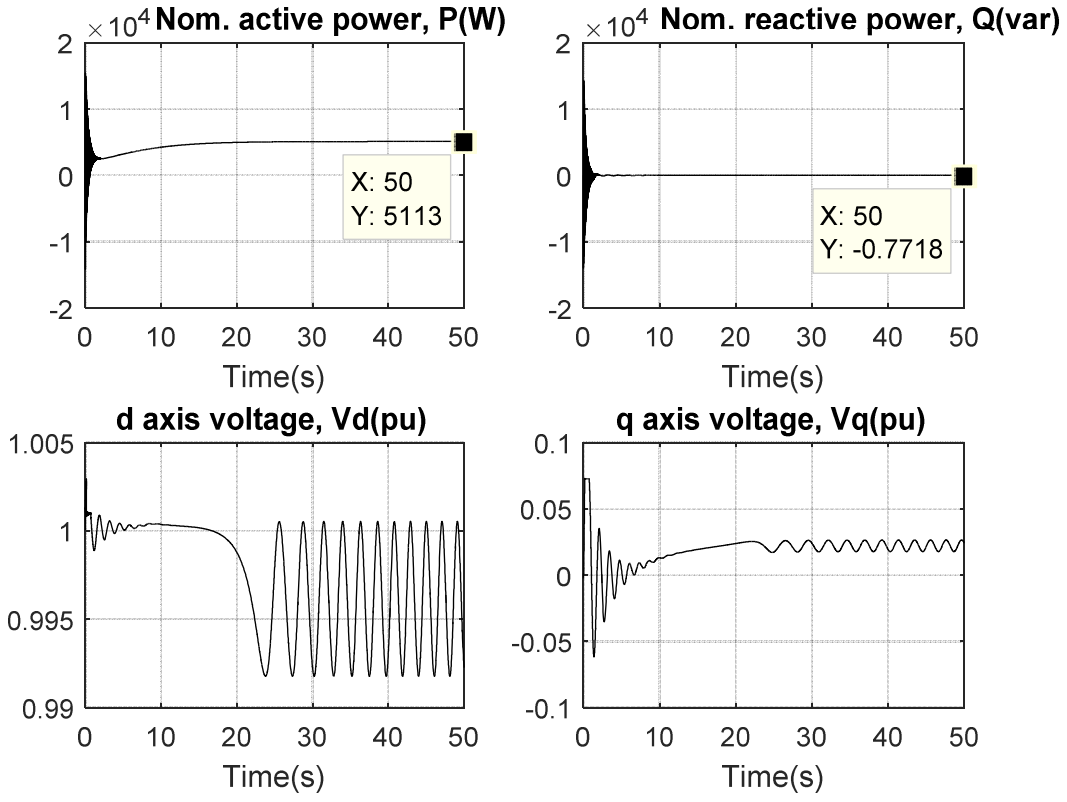

Figure 9(b). *Response of MS2 when terminals of MS1 are short-circuited at 6.0s to 8.0s - Q Control.*

Figure 10(a) and Figure 10(b) present responses of feeder-a to faults at terminals of MS1 under *V* and *Q* controls, respectively.

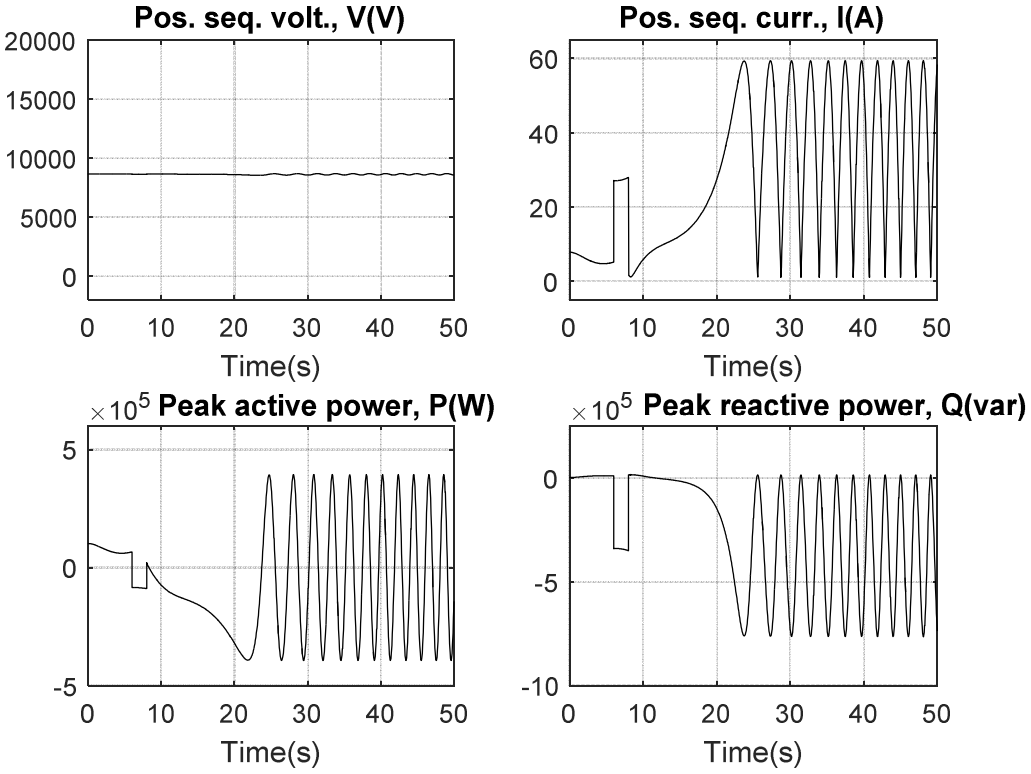

Figure 10(a). *Response of feeder-a when terminals of MS1 are short-circuited at 6.0s to 8.0s - V Control.*

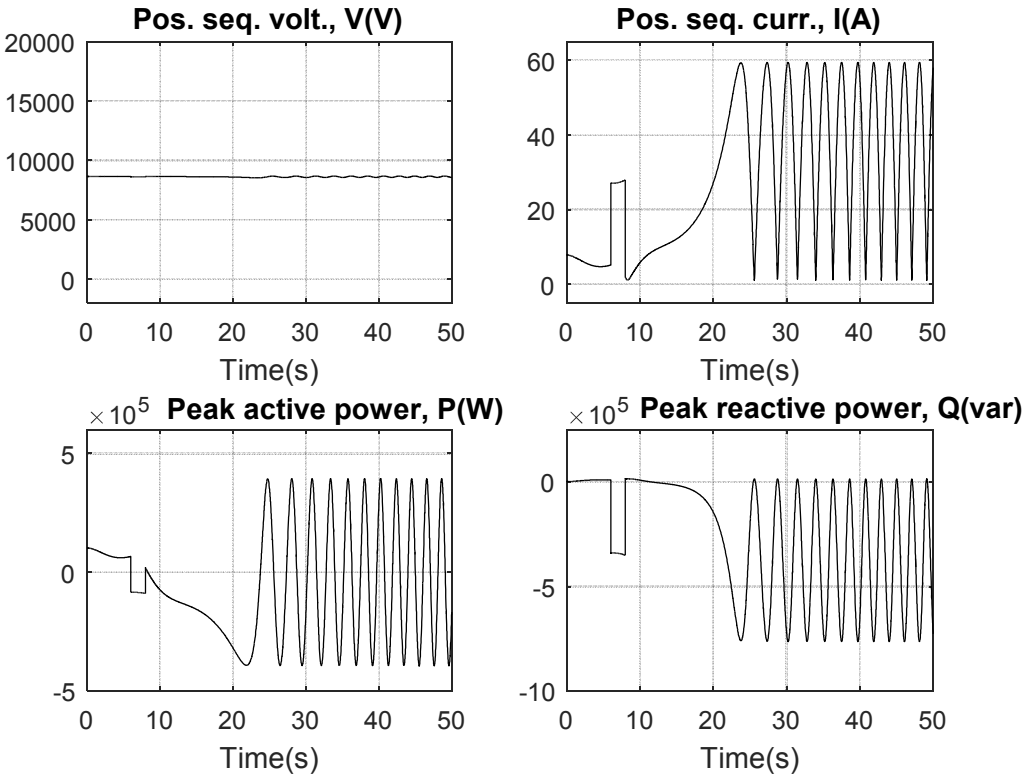

Figure 10(b). *Response of feeder-a when terminals of MS1 are short-circuited at 6.0s to 8.0s - Q Control.*

The responses of MS1 under *V* and *Q* controls when three phase bolted cross-country short circuits are applied at terminals of MS1 and MS2 are presented in Figure 11(a) and Figure 11(b), respectively.

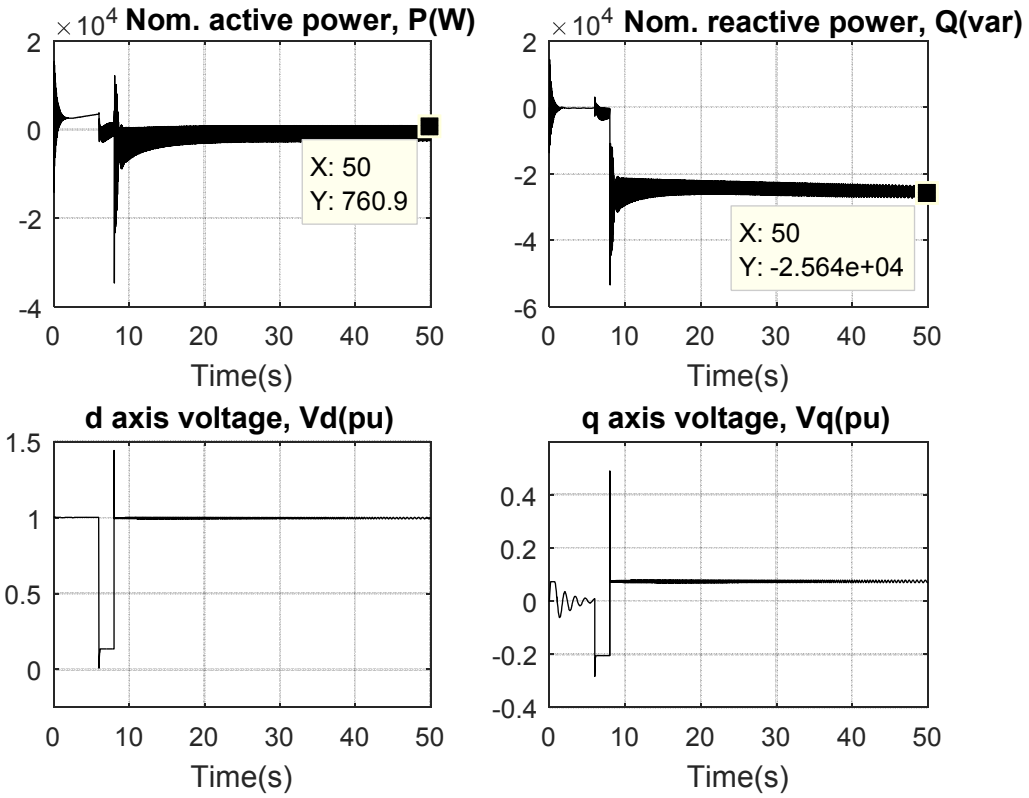

Figure 11(a). *Response of MS1 to a cross-country short circuit at its terminals and terminals of utility generator at 6.0s to 8.0s - V Control.*

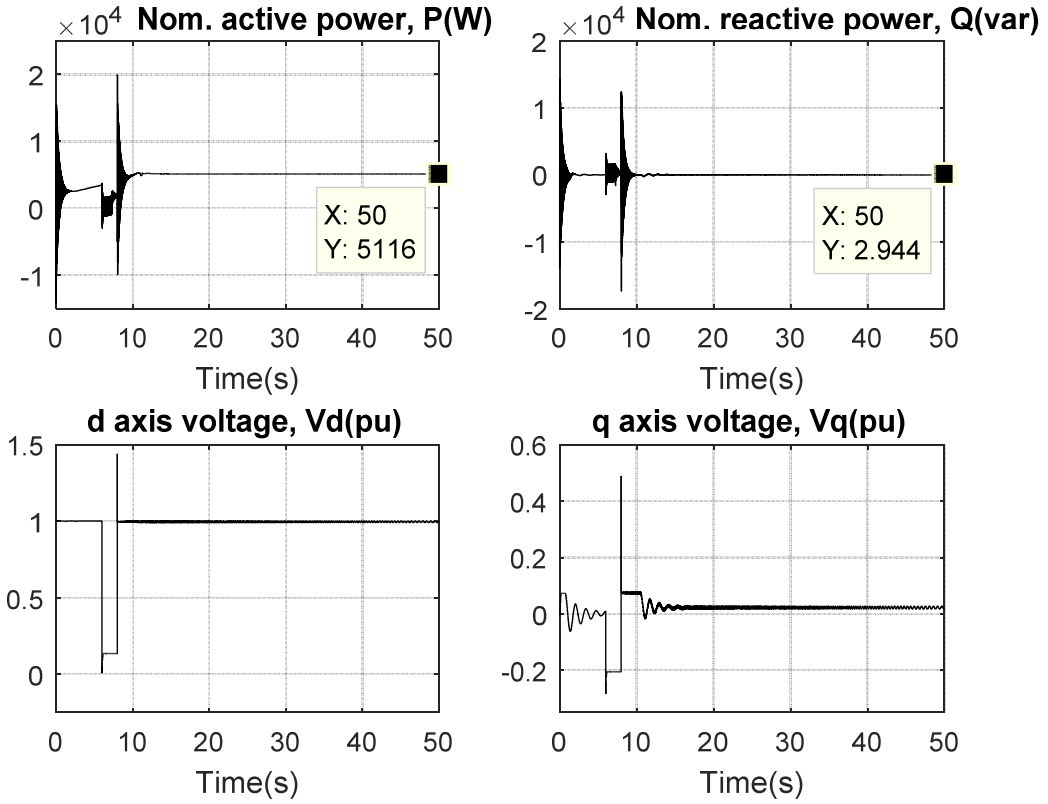

Figure 11(b). *Response of MS1 to a cross-country short circuit at its terminals and terminals of utility generator at 6.0s to 8.0s - Q Control.*

Figure 12(a) and Figure 12(b) present responses of feeder-a when three phase bolted cross-country short circuits are applied at terminals of MS1 and MS2 under *V* and *Q* controls, respectively.

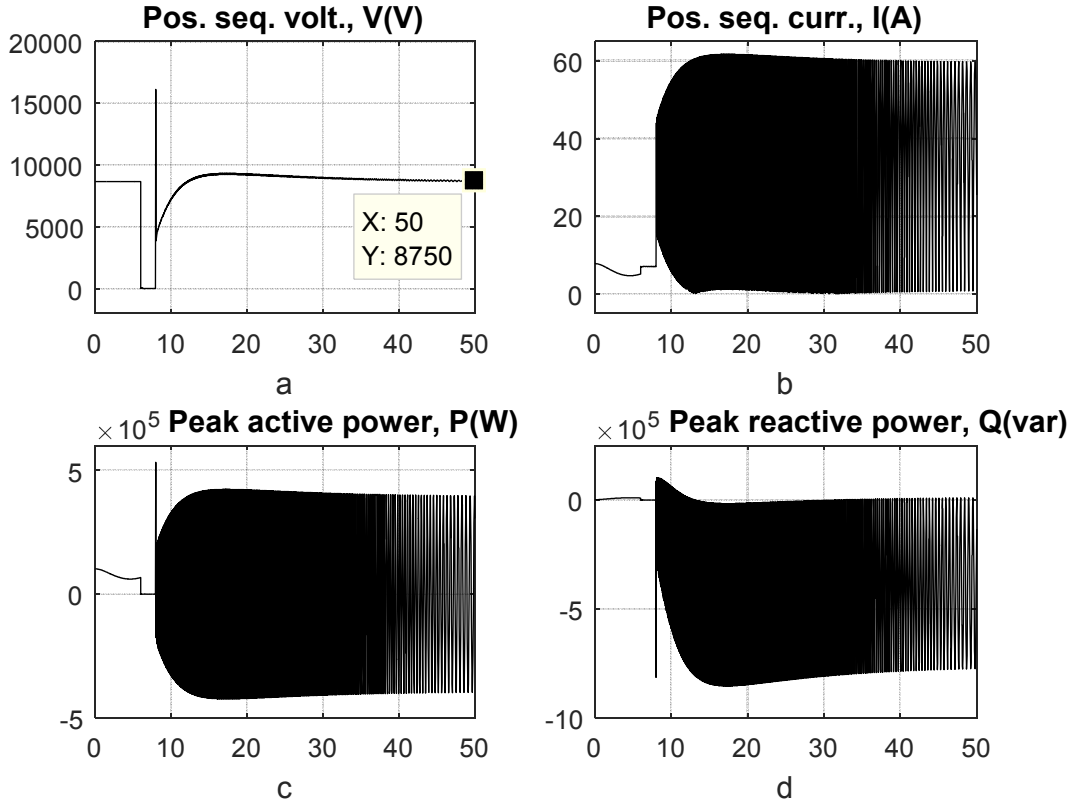

Figure 12(a). *Response of feeder-a to cross-country short circuit at MS1 terminals and terminals of utility generator at 6.0s to 8.0s - V Control.*

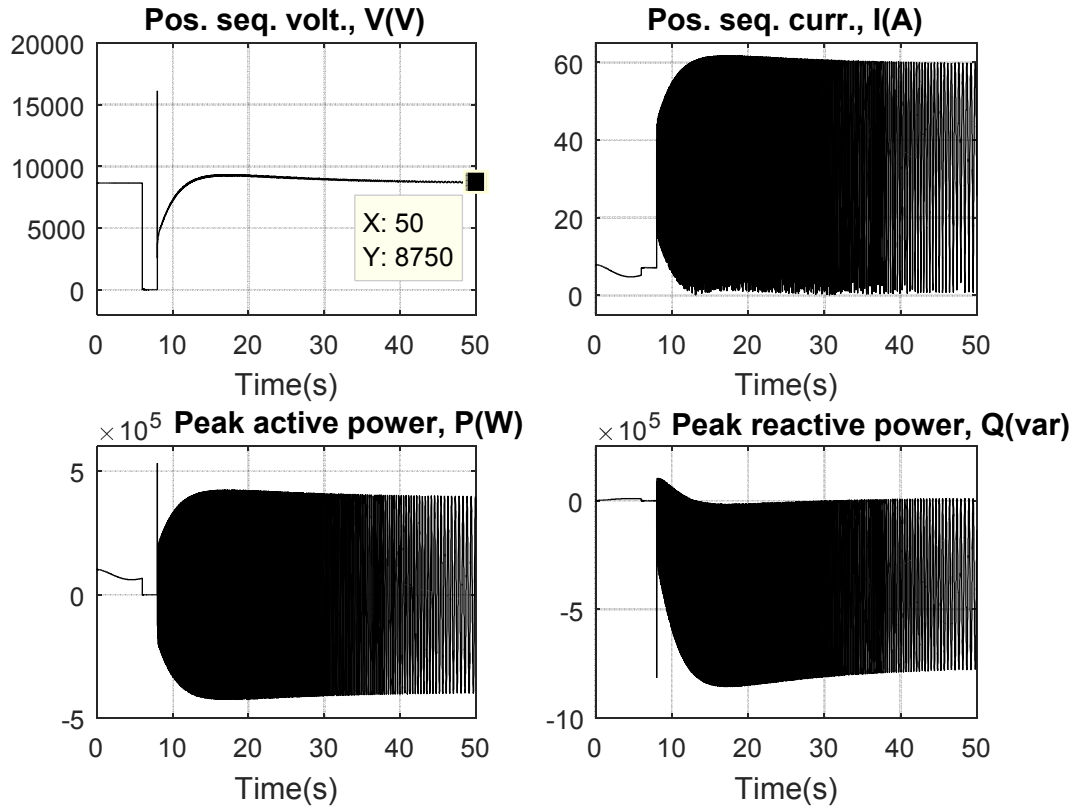

Figure 12(b). *Response of feeder-a to cross-country short circuit at MS1 terminals and terminals of utility generator at 6.0s to 8.0s - Q Control.*

5. Results and Discussions

From the results of the simulation, either of the micro-sources in the micro-grid generates 92% of its nominal rating when the system is free of stress. Also, when operating conditions are normal, either micro-source absorbs more reactive power from the external reactive power compensator under *V* control than *Q* control - indicating reactive support from its converter dc bus under *Q* control [23]. However, this is not sustainable for continuous operation as this support is limited to the small capacity of the converter capacitor linked to its dc bus.

At 50.0s, under *V* control (Figure 4(a)), MS1 generates 5.105kW and contributes 1.376kvar to the short circuit at utility generator terminals. Under *Q* control, it generates 5.116kW and contributes only 2.953var to the same short circuit (Figure 4(b)). This is consistent with the power management capability of DFIG as published by Moayed Moghbel et al. in [24] and in [25, 26]. Because the utility is tied to the micro-grid, the high-magnitude utility short circuit results in post-fault voltage oscillation in the micro-sources and power instability in the feeders, as shown in Figure 4(a) to Figure 5(b). Post-fault instability is a major challenge of micro-grid, as published in [8, 27, 28].

At 50.0s, under *V* control (Figure 6(a)), MS1 generates 5.106kW and contributes 0.8823kvar to utility fault at the end of transmission lines (closer to the micro-grid). Under *Q* control, it generates 5.114kW and contributes only 0.003609kvar to the same short circuit (Figure 6(b)). This shows superior reactive power management capability of DFIG under *Q* control as published by Moayed Moghbel et al. in [24] and in [29, 30]. Because the micro-grid is grid-connected, the high-magnitude utility short circuit provokes post-fault voltage oscillation in the micro-sources and power instability in the feeders, as shown in Figure 6(a) to Figure 7(b). This is a major challenge of micro-grid operation, as published in [31-33].

At 50.0s, under *V* control (Figure 8(a)), MS1 absorbs 0.595kW from MS2 and utility while it absorbs 27.87kvar from both sources when three phase bolted short circuit is applied at its terminals. For the same short circuit condition under *Q* control, it generates 5.113kW but absorbs only 0.8599var from both sources (Figure 8(b)). This validates the reactive power management capability of DFIG as reported by Moayed Moghbel et al. in [24] and in [25, 26, 34]. Because the simulated fault is a three phase bolted short circuit, it provokes post-fault voltage and power instability in the micro-grid, as shown in Figure 8(a) to Figure 10(b). However, because it is a micro-grid short circuit (not utility short circuit), severity of resultant oscillation is not as virulent as obtainable in utility short circuit (Figure 4(a) to Figure 7(b)).

At 50.0s, under *V* control (Figure 11(a)), MS1 generates 0.7609kW but absorbs 25.64kvar from MS2 and utility when the system experiences cross-country three phase bolted short circuit. Under *Q* control, it generates 5.116kW and contributes only 2.944var to the same short circuit (Figure 11(b)). This is consistent with the power management capability of DFIG as published by Moayed Moghbel et al. in [24] and in [25, 26, 34].

Because the simulated fault is a cross-country three phase bolted short circuit, it provokes virulent post-fault voltage and power instability in the micro-grid, as shown in Figure 11(a) to Figure 12(b).

6. Conclusion

When the system is stressed with a 2-second bolted short circuit, the study has shown that power flow between micro-grid and utility is bidirectional, particularly reactive power support at short circuit points. It has also been shown in this work that utility short circuit provokes post-fault sustained virulent power oscillation in the micro-grid feeder due to comparatively lower inertia of the micro-sources and small converter capacities of DFIG to support post-fault power recovery. In this research work, it has been verified that the micro-sources offer better voltage and power post-fault stability under *Q* control than *V* control, when the micro-grid is short-circuited (this is particularly depicted in Figure 8(a) and Figure 8(b); and Figure 9(a) and Figure 9 (b)). Similarly, when the system experiences cross-country short circuits, the results of the simulation have shown that the micro-sources present superior performance under *Q* control than *V* control (this is particularly depicted in Figure11(a) and Fig.11 (b)). Finally, it has been shown that the impact of the cross-country short circuit on the micro-grid is so severe under *V* control that it forces the wind turbine generator to compromise its nominal output active power generation, resulting in sustained oscillations, as depicted in Figure11(a) and Figure 11(b). The reactive power from the utility and capacitive var compensators also experience sustained oscillation. In conclusion, the response of the test bed to balanced three phase bolted short circuit has been shown to be consistent with established theory, validating its response to balanced three phase bolted short circuit.

Abbreviations

MS1 = Micro-source 1, MS2 = Micro-source 2, Feeder-a = Feeder connected to micro-source 1, Feeder-b = Feeder connected to micro-source 2.

References

[1] Coffele, F., et al., Quantitative analysis of network protection blinding for systems incorporating distributed generation. IET Generation, Transmission & Distribution, 2012. 6 (12): p. 1218-1224.

[2] Adio, O. S., et al. Short circuit analysis for integration of 10MW Windfarm in Nigeria at the PCC. in 2013 IEEE Power and Energy Society General Meeting (PES). 2013.

[3] Rona, B. and Ö. Güler, Power system integration of wind farms and analysis of grid code requirements. Renewable and Sustainable Energy Reviews, 2015. 49: p. 100-107.

[4] Samaan, N., et al. Modeling of wind power plants for short circuit analysis in the transmission network. in 2008 IEEE Transmission and Distribution Conference and Exposition. 2008.

[5] Hatziargyriou, N., et al., Microgrids. IEEE Power and Energy Magazine, 2007. 5 (4): p. 78-94.

[6] Jan Machowski, Janusz W. Bialek, and J. R. Bumby, Power System Dynamics and Stability. 1997, England: John Wiley & Sons.

[7] Lasseter, R. H. MicroGrids. in 2002 IEEE Power Engineering Society Winter Meeting. 2002.

[8] Best, R. J., D. J. Morrow, and P. A. Crossley, Current transients in the small salient-pole alternator during sudden short-circuit and synchronisation events. IET Electric Power Applications, 2010. 4(9): p. 687-700.

[9] Chaudhary, M., S. M. Brahma, and S. J. Ranade. Validated short circuit modeling of Type 3 Wind Turbine Generator with crowbar protection. in North American Power Symposium (NAPS), 2013. 2013.

[10] Dos Santos, A. and M. T. C. d. Barros, Stochastic modeling of power system faults. Electric Power Systems Research, 2015. 126: p. 29-37.

[11] Haoen, L., A. Bose, and Z. Yang, On-line short-circuit current analysis and preventive control to extend equipment life. IET Generation, Transmission & Distribution, 2013. 7 (1): p. 69-75.

[12] Kersting, W. H. and G. Shirek. Short circuit analysis of IEEE test feeders. in 2012 IEEE PES Transmission and Distribution Conference and Exposition (T & D) 2012.

[13] Prajapati, J., V. Patel, and H. Patel. Load flow, short circuit and stability analysis using Matlab. in 2014 International Conference on Green Computing Communication and Electrical Engineering (ICGCCEE). 2014.

[14] Roennspiess, O. E. and A.E. Efthymiadis, A comparison of static and dynamic short circuit analysis procedures. IEEE Transactions on Industry Applications, 1990. 26(3): p. 463-475.

[15] Salon, S. J., et al. Short circuit analysis of large doubly-fed induction generators. in 2013 IEEE International Electric Machines & Drives Conference (IEMDC). 2013.

[16] Soni, N., S. Doolla, and M.C. Chandorkar, Improvement of Transient Response in Microgrids Using Virtual Inertia. IEEE Transactions on Power Delivery, 2013. 28(3): p. 1830-1838.

[17] Sulla, F., J. Svensson, and O. Samuelsson, Symmetrical and unsymmetrical short-circuit current of squirrel-cage and doubly-fed induction generators. Electric Power Systems Research, 2011. 81 (7): p. 1610-1618.

[18] Bracale, A., et al. Probabilistic short circuit analysis in electric power distribution systems including distributed generation. in 8th Mediterranean Conference on Power Generation, Transmission, Distribution and Energy Conversion (MEDPOWER 2012). 2012.

[19] Jen-Hao, T., Unsymmetrical Short-Circuit Fault Analysis for Weakly Meshed Distribution Systems. IEEE Transactions on Power Systems, 2010. 25(1): p. 96-105.

[20] Ouyang, J. and X. Xiong, Dynamic behavior of the excitation circuit of a doubly-fed induction generator under a symmetrical voltage drop. Renewable Energy, 2014. 71: p. 629-638.

[21] Aminu, M. A. and K. Solomon, A Review of Control Strategies for Microgrids. Advances in Research, 2016. 7 (3): p. 1-9.

[22] Aminu, M. A., Design of Reactive Power and Voltage Controllers for Converter-interfaced ac Microgrids. British Journal of Applied Science & Technology, 2016. 17 (1).

[23] Ferreira de Souza, W.a.S.-M., M. A. and Lopes, L. A. C., Power sharing control strategies for a three-phase microgrid in different operating condition with droop control and damping factor investigation. IET Renewable Power Generation, 2015. 9 (7): p. 831-839.

[24] Moghbel, M., et al. Reactive power control of DFIG wind power system connected to IEEE 14 bus distribution network. in Universities Power Engineering Conference (AUPEC), 2012 22nd Australasian. 2012.

[25] Mehdi, A., et al. Direct active and reactive power control of DFIG based wind energy conversion system. in 2014 International Symposium on Power Electronics, Electrical Drives, Automation and Motion (SPEEDAM). 2014.

[26] Pati, S. and S. Samantray. Decoupled control of active and reactive power in a DFIG based wind energy conversion system with conventional P-I controllers. in 2014 International Conference on Circuit, Power and Computing Technologies (ICCPCT). 2014.

[27] Olivares, D. E., et al., Trends in Microgrid Control. IEEE Transactions on Smart Grid, 2014. 5(4): p. 1905-1919.

[28] Soultanis, N. L. and N. D. Hatziargyriou. Control issues of inverters in the formation of LV microgrids. in 2007 IEEE Power Engineering Society General Meeting. 2007.

[29] Gopalan, S. A., V. Sreeram, and H. H. C. Iu, A review of coordination strategies and protection schemes for microgrids. Renewable and Sustainable Energy Reviews, 2014. 32: p. 222-228.

[30] Planas, E., et al., General aspects, hierarchical controls and droop methods in microgrids: A review. Renewable and Sustainable Energy Reviews, 2013. 17: p. 147-159.

[31] Romo, R. and O. Micheloud, Power quality of actual grids with plug-in electric vehicles in presence of renewables and microgrids. Renewable and Sustainable Energy Reviews, 2015. 46: p. 189-200.

[32] Soshinskaya, M., et al., Microgrids: Experiences, barriers and success factors. Renewable and Sustainable Energy Reviews, 2014. 40: p. 659-672.

[33] Zamora, R. and A.K. Srivastava, Controls for microgrids with storage: Review, challenges, and research needs. Renewable and Sustainable Energy Reviews, 2010. 14(7): p. 2009-2018.

[34] Vinothkumar, K. and M.P. Selvan. Enhanced fault ride-through scheme and coordinated reactive power control for DFIG. in 2010 IEEE International Conference on Sustainable Energy Technologies (ICSET). 2010.